COLO HEP 428

Detecting the Two Photon Background for Supersymmetry in the Midst of a Large Beamstrahlung Background.

Nick Danielson and Bonna Newman

August 15, 2000

1 Introduction

It recently became a concern that the two photon process poses a problem for the study of Supersymmetry because it mimics certain Supersymmetric signals [1, 2]. One method of discerning between two photon events and Supersymmetric events is to put a detector at low angles (approximately 40 mrad or less) to the beam axis in order to detect at least one of the two high energy electrons present in two photon events. However, at such low angles there may be primary beam particles, bremsstrahlung, beamsstrahlung, and the consequent pair-produced electrons and positrons that can cause problems for a detector for two reasons: (1) If this radiation is too intense, it may actually destroy the detector. (2) It may be difficult to discriminate between the one or two electrons and positrons generated in two photon events and the many unwanted particles that come from beam interactions.

In this paper this intense radiation is analyzed with the beam-beam interaction simulation program Guinea Pig [3]. Although primary beam particles and photons from bremsstrahlung and beamsstrahlung most likely will not hamper the identification of two photon events because they are in the extreme forward direction, the pair-produced particles associated with these forward photons have sufficient intensity and large enough angles to pose a problem.

2 Discussion of two photon events

In a typical two photon event ($e^+e^- \to e^+e^-\gamma^*\gamma^* \to e^+e^-e^+e^-$), two electrons and two positrons are present in the final state. Equally, we can also have the final states $e^+e^-\mu^+\mu^-$, $e^+e^-q\overline{q}$ (hadrons), and $e^+e^-W^+W^-$. If all four of these particles are observed, the event can be recognized as a two photon event. However, often one electron and one positron are deflected only slightly and travel at low angles relative to the beam axis. These two high-energy electrons can be lost down the beam pipe, carrying energy away. However, because they are nearly back to back, they carry away very little net transverse momentum. The remaining signature in the detector—one electron, one positron, large missing energy, and low transverse momentum—often allows these events to be eliminated easily. However, studies [1, 2] have shown that this signature may actually mimic some Supersymmetric signals, since there are large amounts of missing energy in Supersymmetric events, too. Hence there is a need to tag this background to separate it from the Supersymmetric signal. A previous study [1] has shown that if a detector can be installed at low angles (approximately 40 mrad or less) to the beam axis to see high-energy, low-angle particles, then this two photon background can be greatly reduced. The study that indicated that 40 mrad would be sufficient was looking at point 2 Supersymmetric data. In order to allow for different Supersymmetric models, we need to see to lower angles such as 20 or 30 mrad. As mentioned above, two impediments to this method are that at these low angles the particles produced by the beamstrahlung may drown out the signal from the high-energy electron and positron that come from a two photon event or may even damage the detector because of the intense ratdiation.

3 Accelerator parameters

The data in this paper were generated with the program Guinea Pig [3]. Guinea Pig was configured to simulate the NLC running at 500 GeV center of mass energy with the machine design parameters shown in Table 1.

Table 1: Machine design parameters input to Guinea Pig to simulate the NLC running at a center of mass energy of 500 GeV. These parameters were taken from the Guinea Pig homepage at http://www-sldnt.slac.stanford.edu/nlc/guinea_pig.htm and are similar to those described in [4]. Their meanings are discussed in more detail in [3].

Beam energy (GeV)	245
Number of particles per bunch	$.95 \times 10^{10}$
$\gamma\epsilon_x/\gamma\epsilon_y$ at interaction point (μm)	4.5/.1
β_x/β_y at interaction point (mm)	12/.12
σ_x/σ_y at interaction point (nm)	330/4.9
σ_z at interaction point (mm)	120
Energy spread	.3%
Energy spread distribution	delta function
Travelling Focus (hourglass effect)	OFF
Initial state radiation (do_isr)	ON
do_espread	ON
Bremsstrahlung (do_compt)	ON
do_lumi	ON
Minimum energy of pair-produced e^+e^- (pair_ecut) (MeV)	5
electron_ratio (0-1)	0.1
photon_ratio (0-1)	0.1
pair_ratio	1.0
lumi_p	0.0001
hadron_ratio	1000
jet_ratio	10000
Minimum jet p_T (GeV)	3.2

4 Primary beam particles, bremsstrahlung, beamsstrahlung, and bhabha events

Figure 1 illustrates the angular distribution of primary beam particles and photons from bremsstrahlung and beamsstrahlung. The vast majority of particles are confined to an angular region of 0.5 mrad, and thus most likely will not present a problem to a detector situated tens of mrad from the beam axis.

When an electron and positron simply scatter off of each other without producing any other particles, we call this a bhabha event. As Figure 2 shows, particles in these events scatter at such low angles that they also should not pose a problem for us. In fact the bhabha cross section is less than the two photon cross section at 500 GeV.

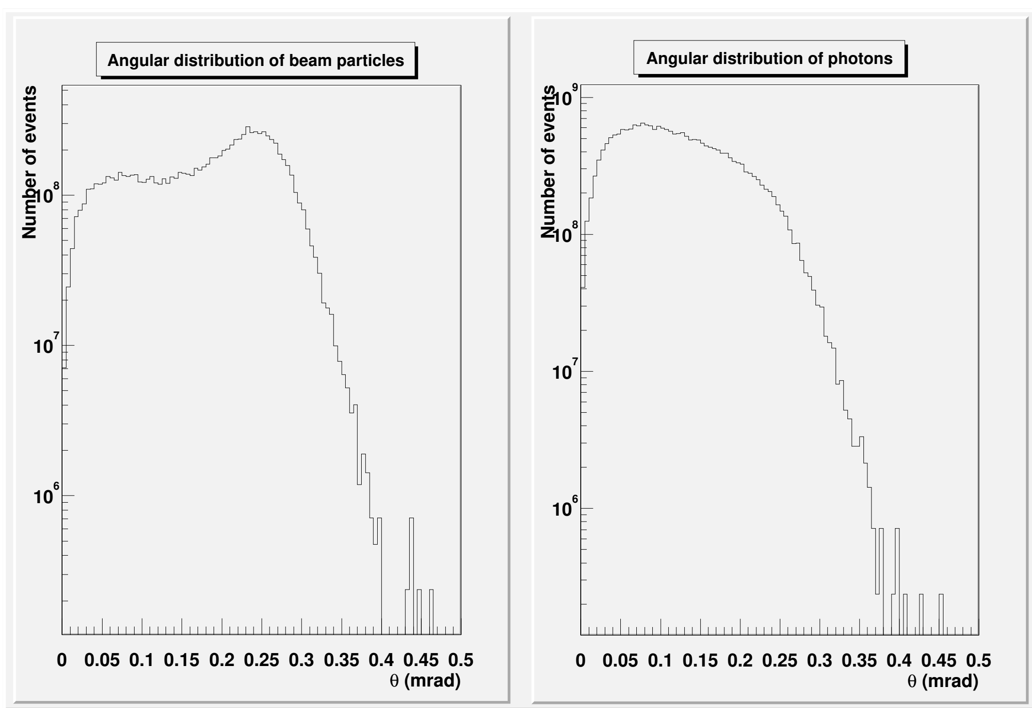

Figure 1: The angle of the beam particles and photons relative to the beam axis after the interaction point. This has been scaled to represent one bunch.

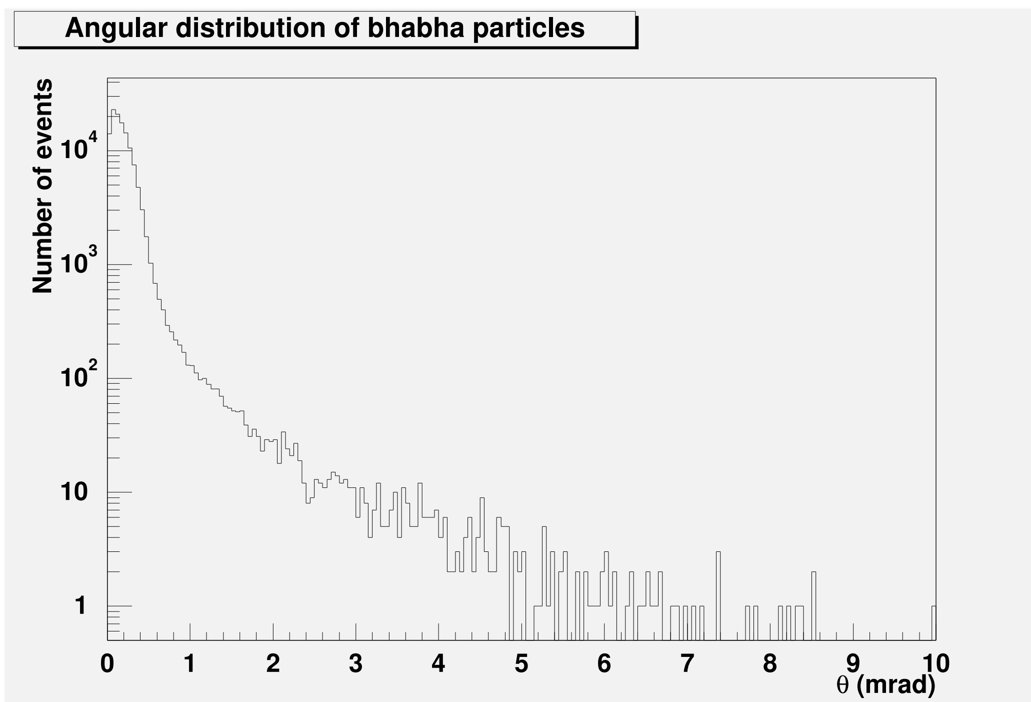

Figure 2: The angle of bhabha particles relative to the beam axis after the interaction point. This chart is unnormalized.

5 Pair-produced particles

The photons radiated by the beam can produce electrons and positrons which travel at large angles as Figure 3 demonstrates. In order to determine if the large number of these particles is enough to destroy a detector, we must look at the energy deposited per cm^2. The particles' trajectories depend on the strength of the magnetic field used. Figure 4 shows the energy deposited per cm^2 per bunch crossing. This is the energy in GeV that is present 150 cm from the interaction point. The radius refers to the distance in the x-y plane.

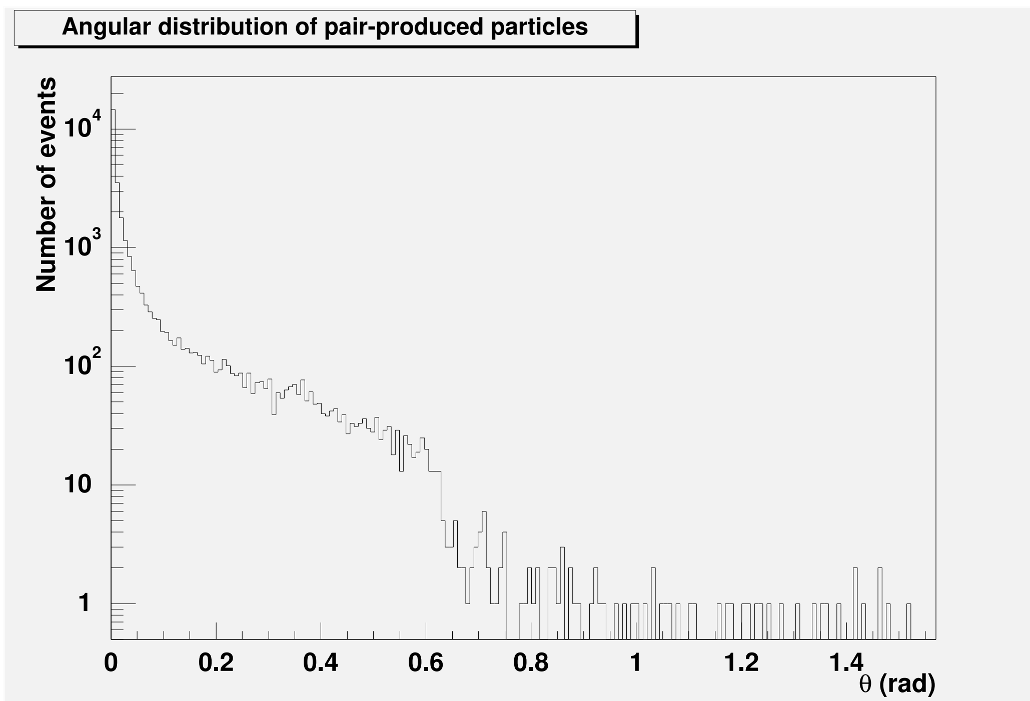

Figure 3: The angle relative to the beam axis of pair-produced electrons and positrons.

We also would like to know if a detector can discriminate between the one or two high-energy low-angle electrons produced in two photon events and the multitude of pair-produced particles. If the pair-produced particles have much lower energies than the high energy members of the two-photon electrons, we might be able to detect the two photon process and eliminate

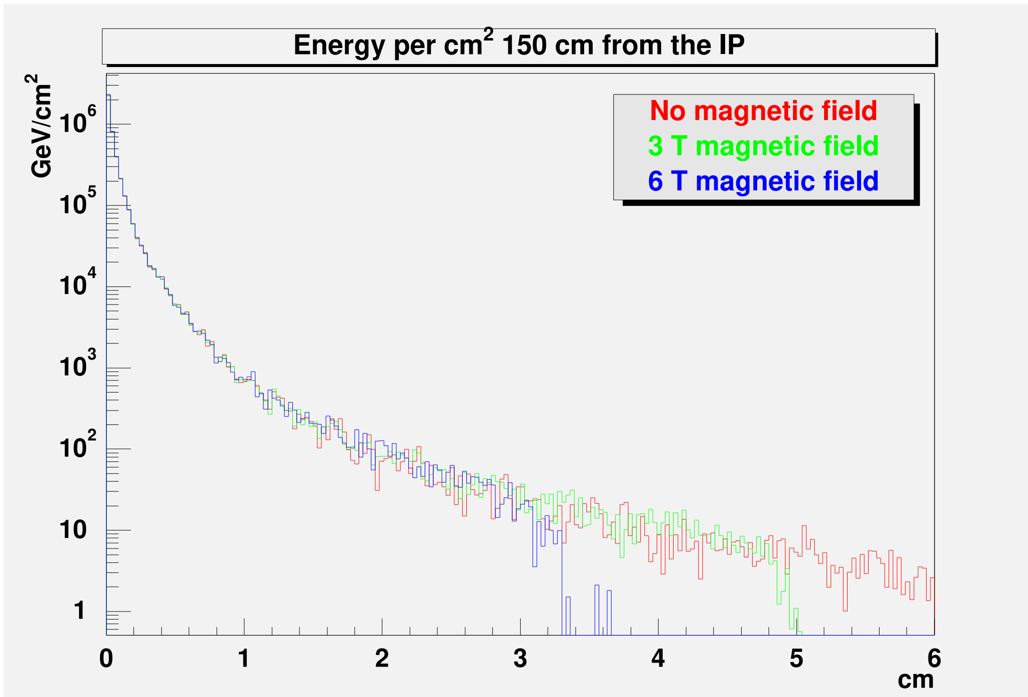

Figure 4: The energy per cm^2 incident on the x-y plane 150 cm from the interaction point when a constant field of 0, 3, and 6 T is added along the z axis. This includes only pair-produced particles.

it as a source of background for Supersymmetric signals.

Figure 5 shows the energy distribution of the electrons and positrons at various radii. In the region of interest (40 mrad, or a radius of about 6 cm), the energies of these particles are only a few GeV. However, each of these figures only represents one bunch of particles (1 bunch = 10^{10} particles). In order to determine the effectiveness of the detector it should be noted that there are 95 bunches per pulse and 120 pulses per second [4]. The response time for the detector is around 20 nanoseconds, during which time 10 bunches of particles will hit the be incident upon the detector. The data in Figure 4 has to be scaled by a factor of ten to correctly represent the energy that the detector will experience.

Note that these plots have assumed a constant magnetic field. A real detector will have a solenoidal magnetic field. In order to study the effects of a real solenoidal magnetic field on our results, a 6 T field has been incorporated into the detector simulation program GEANT[1]. Figure 6 compares the results of a constant 6 T field with the real solenoidal field. This plot shows that there is only a slight difference between the two.

[1] See http://wwwinfo.cern.ch/asdoc/geant_html3/geantall.html for more information

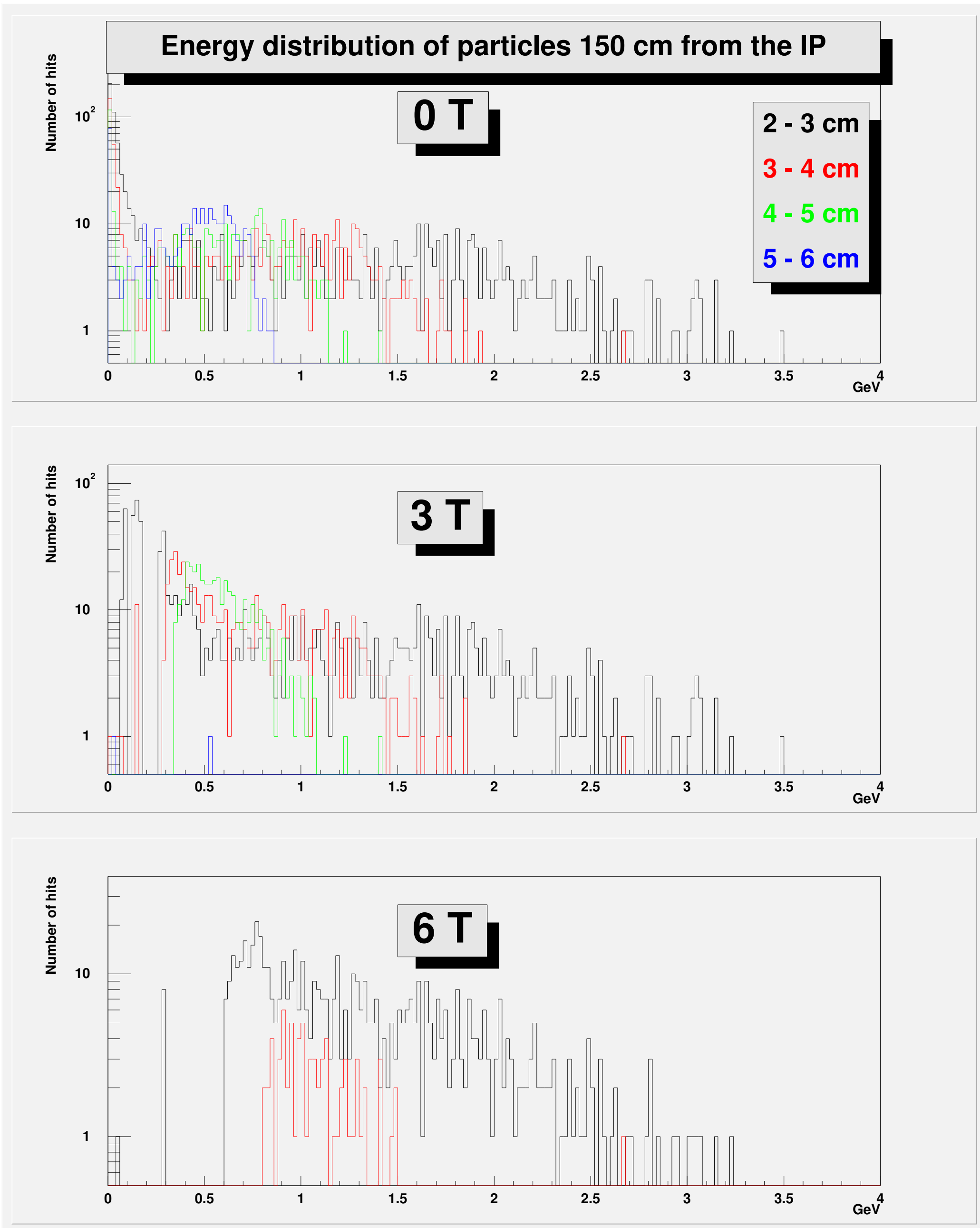

Figure 5: The energy distribution of pair-produced electrons and positrons at various radii in the x-y plane a distance of 150 cm from the interaction point.

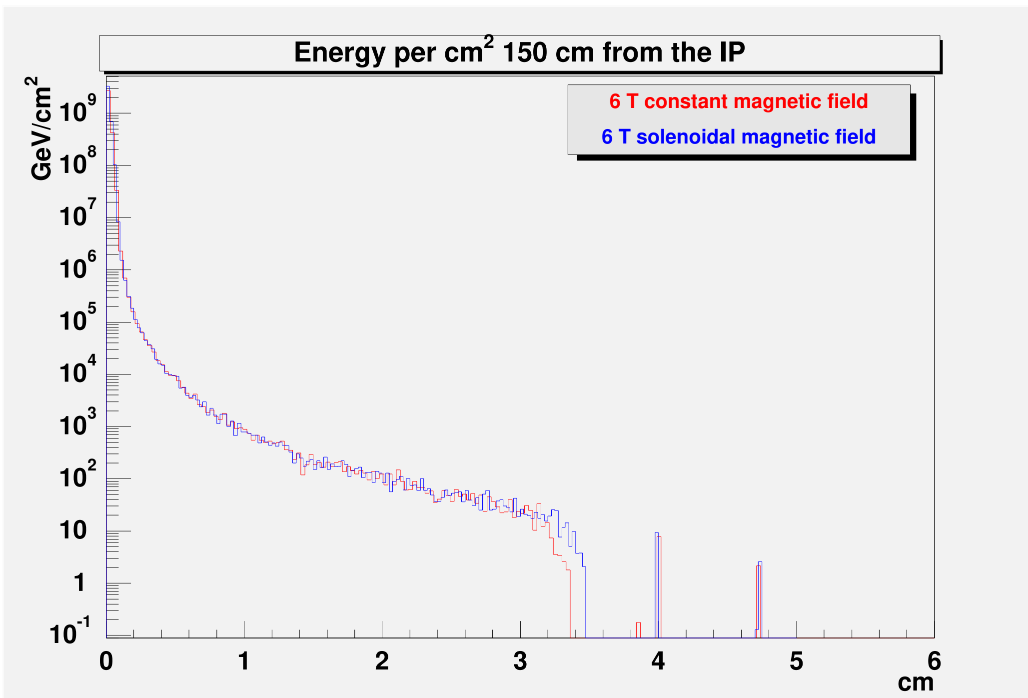

Figure 6: The energy per cm^2 incident on the x-y plane 150 cm from the interaction point when a constant 6 T field or a solenoidal 6 T field is added along the z axis. This includes bhabha particles as well as pair-produced particles.

6 The beam crossing angle

The current NLC design incorporates a 20 mrad beam crossing angle [4]. When the beam crossing angle is taken into account but no magnetic field is applied, the electrons and positrons travel in straight lines so that 150 cm from the interaction point most of them are centered around a point 1.5 cm to the right of the origin of the x-y plane. Once the magnetic field is turned on, the electrons and positrons have curled trajectories, and their distribution 150 cm from the interaction point is no longer azimuthally symmetric. Figure 7 shows the energy distribution of electrons and positrons with and without a 6 T solenoidal field. Figure 8 is the same plot but with more detail in the 100–10^4 GeV/cm^2 region.

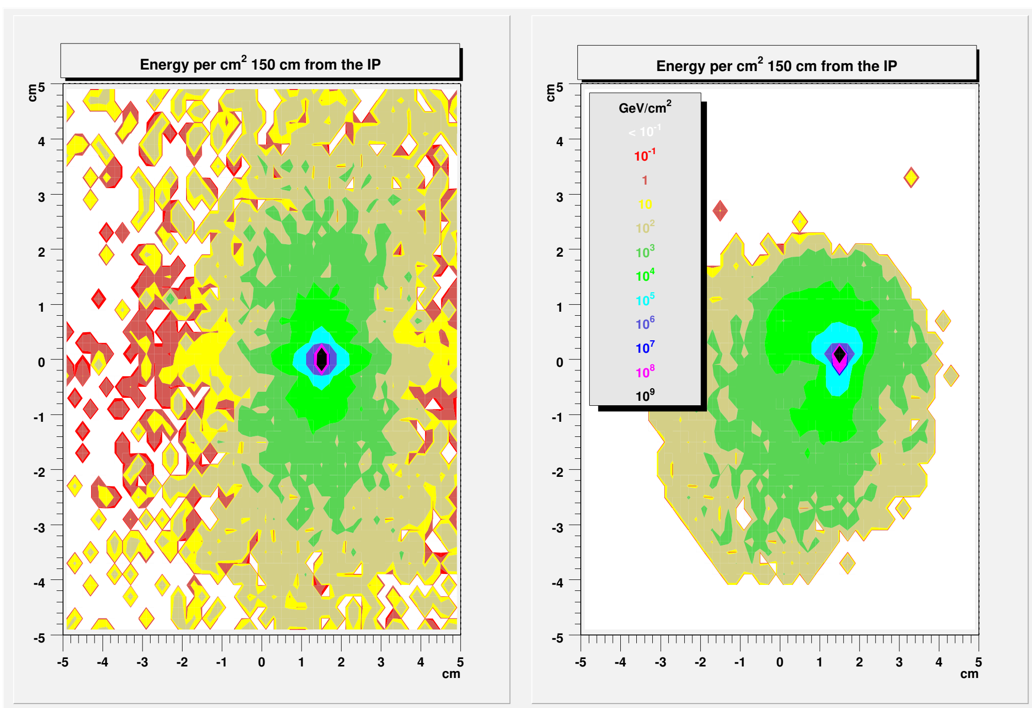

Figure 7: The energy per cm^2 incident on the x-y plane 150 cm from the interaction point. The first plot is without a magnetic field; the second is with a 6 T solenoidal field. The 20 mrad beam crossing angle has been incorporated into these plots.

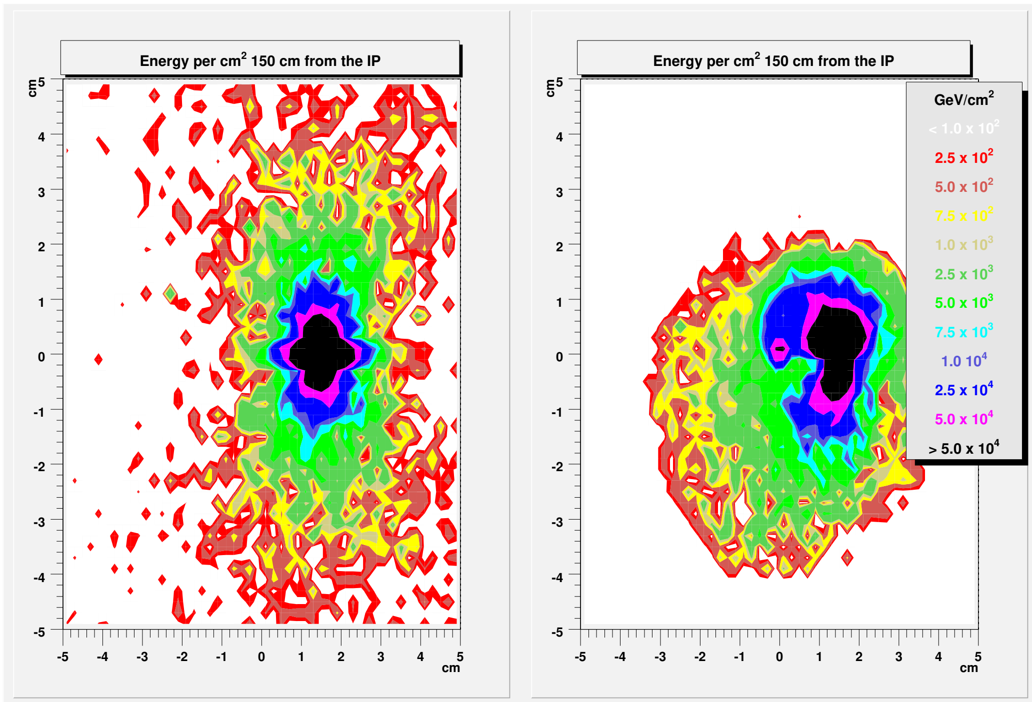

Figure 8: The energy per cm^2 incident on the x-y plane 150 cm from the interaction point. The first plot is without a magnetic field; the second is with a 6 T solenoidal field. The 20 mrad beam crossing angle has been incorporated into these plots.

By convention, the initial electrons travel in the positive z direction while positrons travel in the negative z direction. After the interaction point, pair-produced positrons travelling in the positive direction will we repelled by the magenetic field of the incoming positron beam forming a much more scattered energy distribution. Pair-produced electrons travelling in the positive direction will be attracted by the magnetic field of the incoming positron beam creating a much more concentrated energy distribution. A reverse phenomenon occurs in the negative direction.

In order to see the distribution of energy more cleary, the 2D plots above can be broken into 1D plots of thirty degree segments of phi, or the azimuthal angle. The angle phi is measured from a 0 degree line defined along the positive x-axis as it would be defined in a unit circle. These plots seen in the next 24 figures describe the energy distributed in the positive direction by both electrons and positrons. The energy per centimeter was found by calculating the amount of energy per radial segment divided by the area of that radial segment. These plots are generated with five times as much data scaled to represent one beam particle bunch for better statistical accuracy. As can be seen in Figures 9 through20, the electrons tightly bunched in radius with the greatest amount of energy deposited at approximately 1.5 cm along the positive x direction. Similarly, the positrons, shown in Figures 21 through 32 are more spread out but also with a large distribution of energy at approximately 1.5 cm along the positive x-direction. This shift of the highest concentration from the origin to 1.5 cm in the x direction is caused by the beam crossing angles. Since each beam is incident at 10 mrad to the z-axis at the reaction point, the off axis momentum translates translates into an off-center distribution of the particles in the x-direction carried through by the Lorentz transformations. The total energy deposited here is approximately 3.5 x 10^{10} GeV/cm^2. This energy distribution could make getting a detector at that small of an angle fairly difficult.

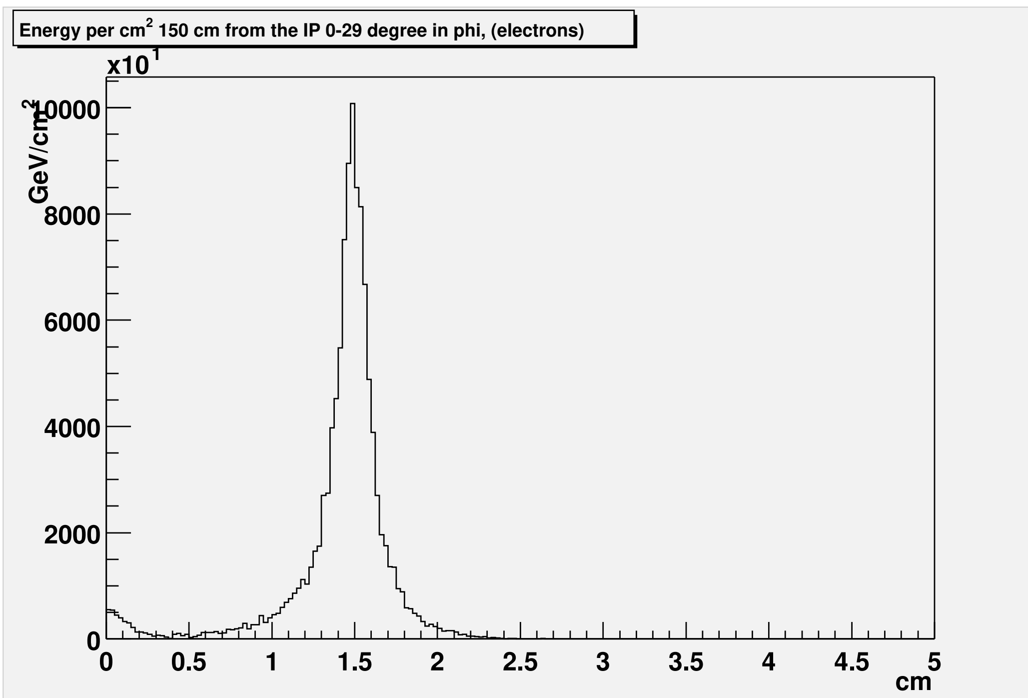

Figure 9: The energy per cm^2 deposited by electrons on a plane 150 cm in the positive direction between 0 and 30 degrees azimuthally.

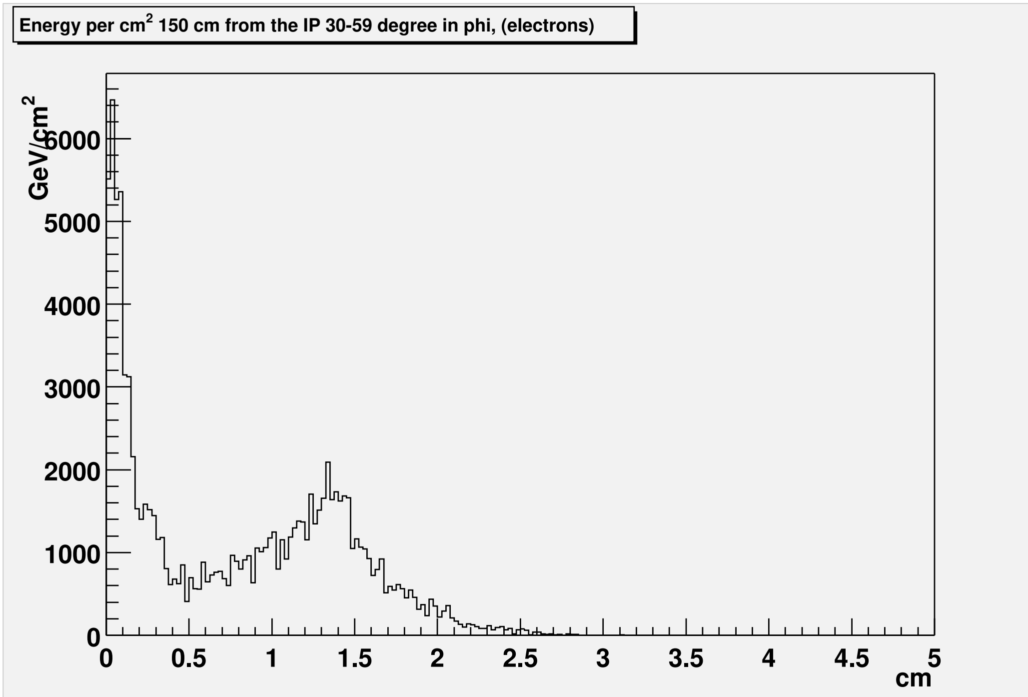

Figure 10: The energy per cm^2 deposited by electrons on a plane 150 cm in the positive direction between 30 and 60 degrees azimuthally.

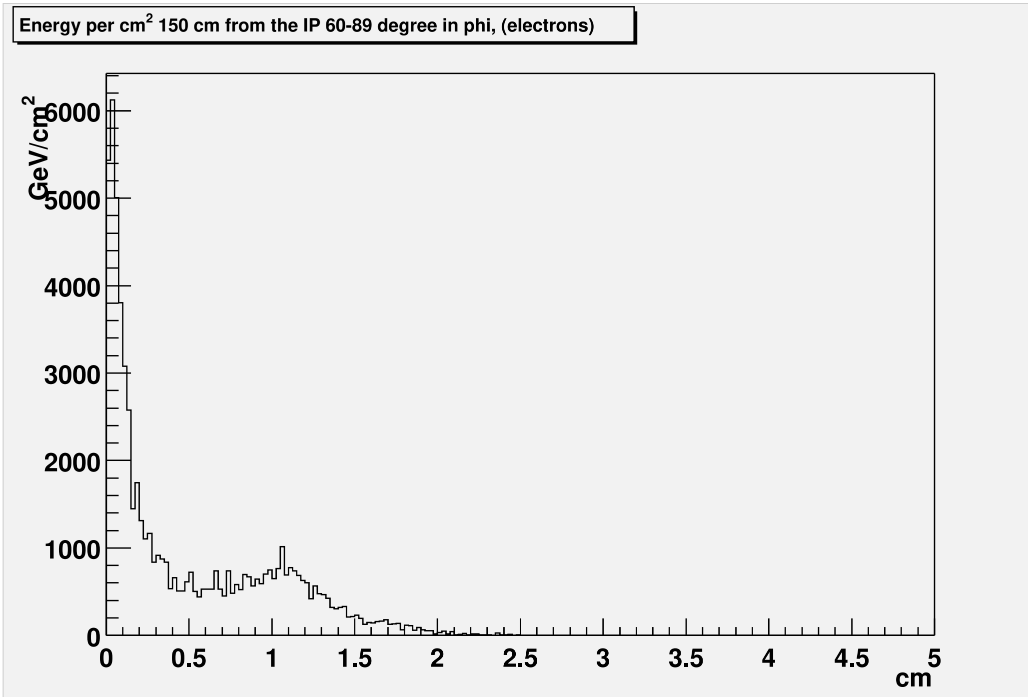

Figure 11: The energy per cm^2 deposited by electrons on a plane 150 cm in the positive direction between 60 and 90 degrees azimuthally.

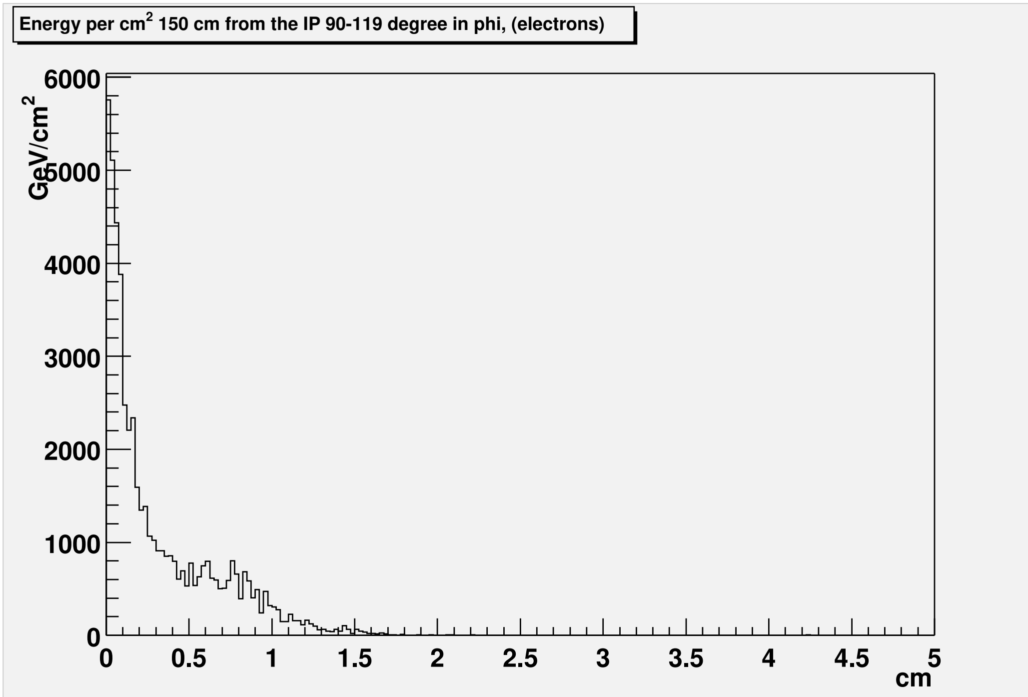

Figure 12: The energy per cm^2 deposited by electrons on a plane 150 cm in the positive direction between 90 and 120 degrees azimuthally.

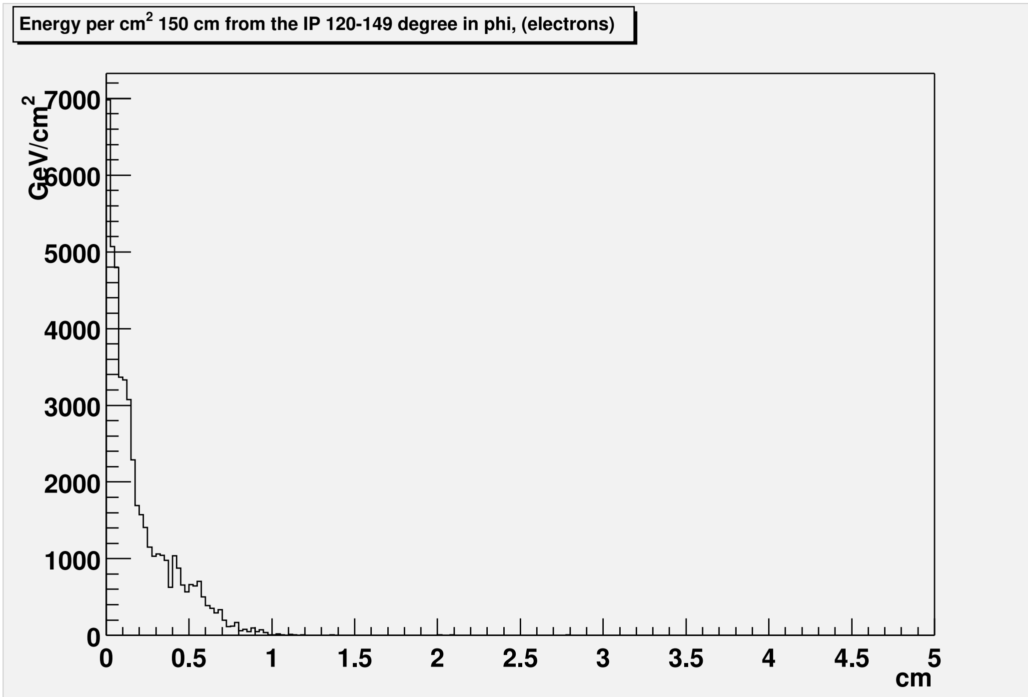

Figure 13: The energy per cm^2 deposited by electrons on a plane 150 cm in the positive direction between 120 and 150 degrees azimuthally.

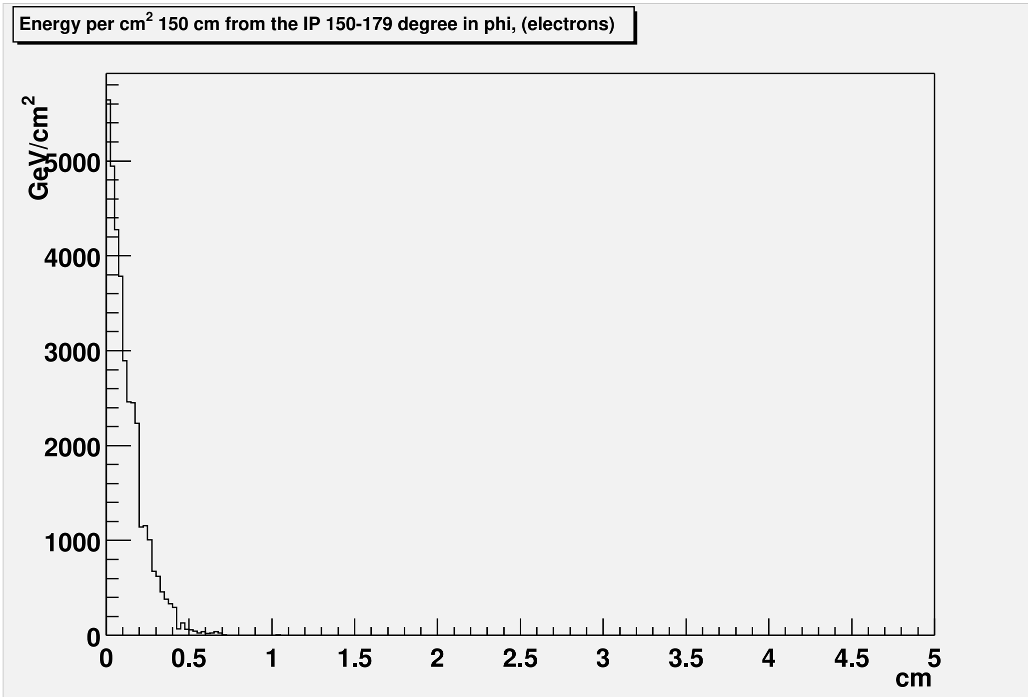

Figure 14: The energy per cm^2 deposited by electrons on a plane 150 cm in the positive direction between 150 and 180 degrees azimuthally.

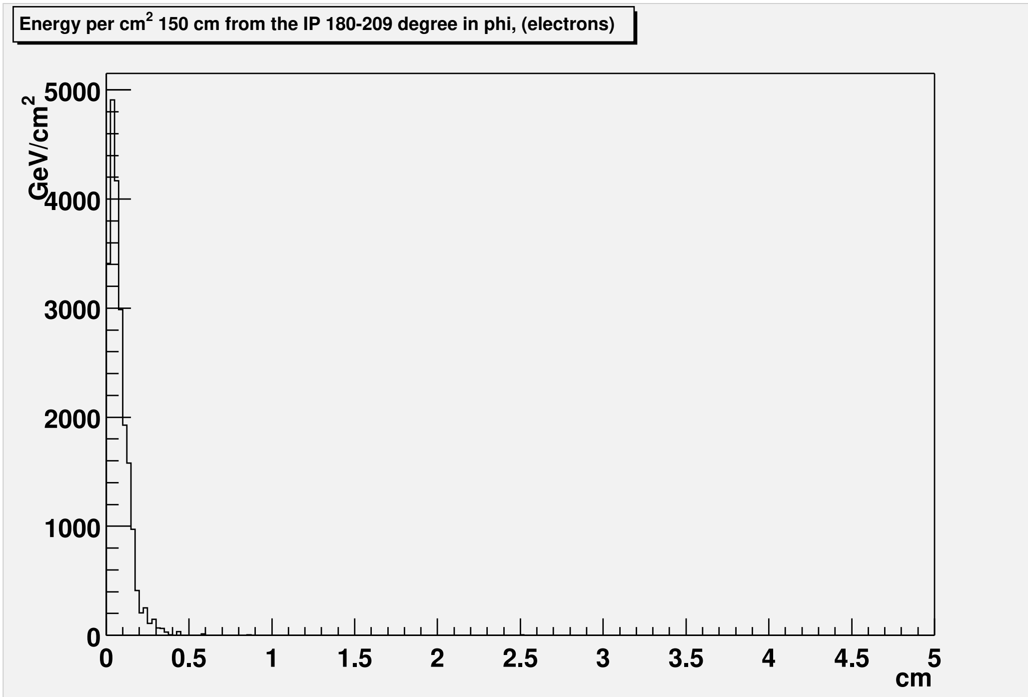

Figure 15: The energy per cm^2 deposited by electrons on a plane 150 cm in the positive direction between 180 and 210 degrees azimuthally.

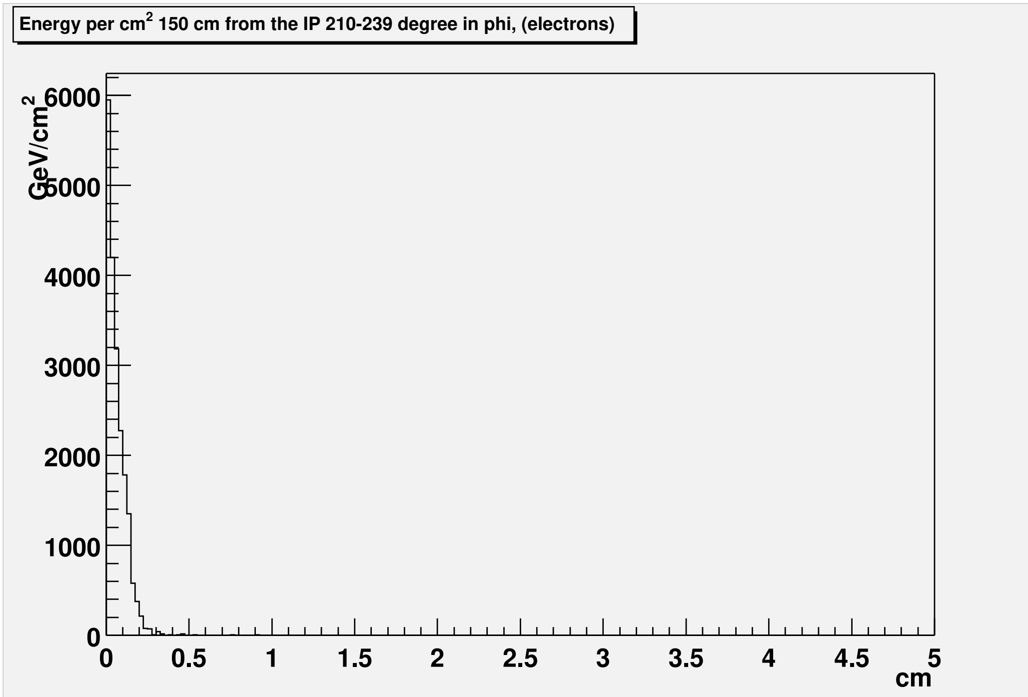

Figure 16: The energy per cm^2 deposited by electrons on a plane 150 cm in the positive direction between 210 and 240 degrees azimuthally.

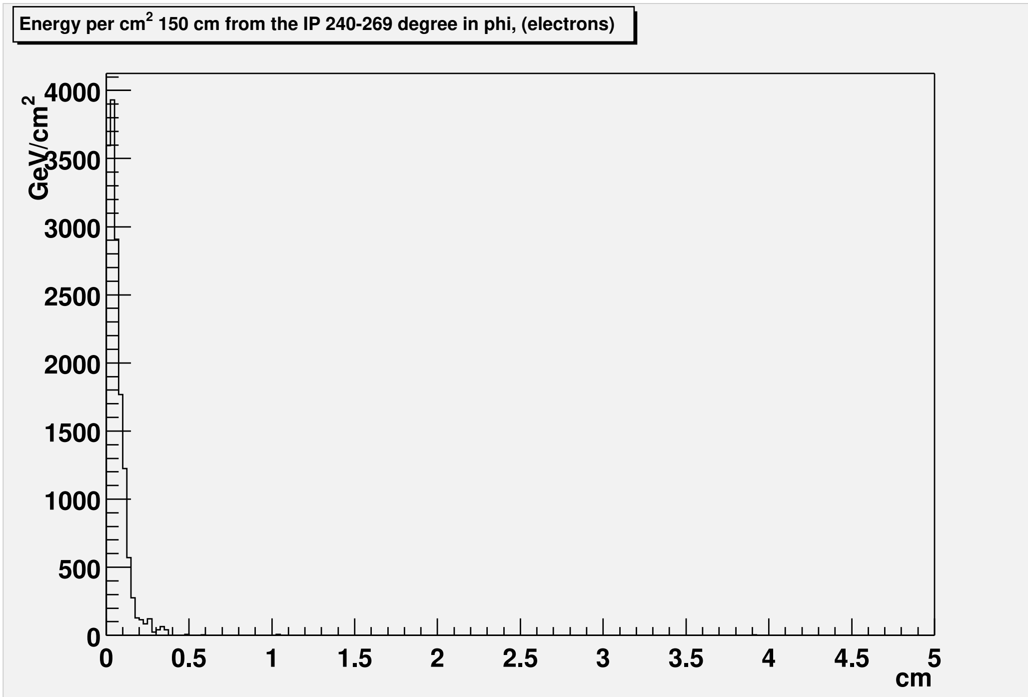

Figure 17: The energy per cm^2 deposited by electrons on a plane 150 cm in the positive direction between 240 and 270 degrees azimuthally.

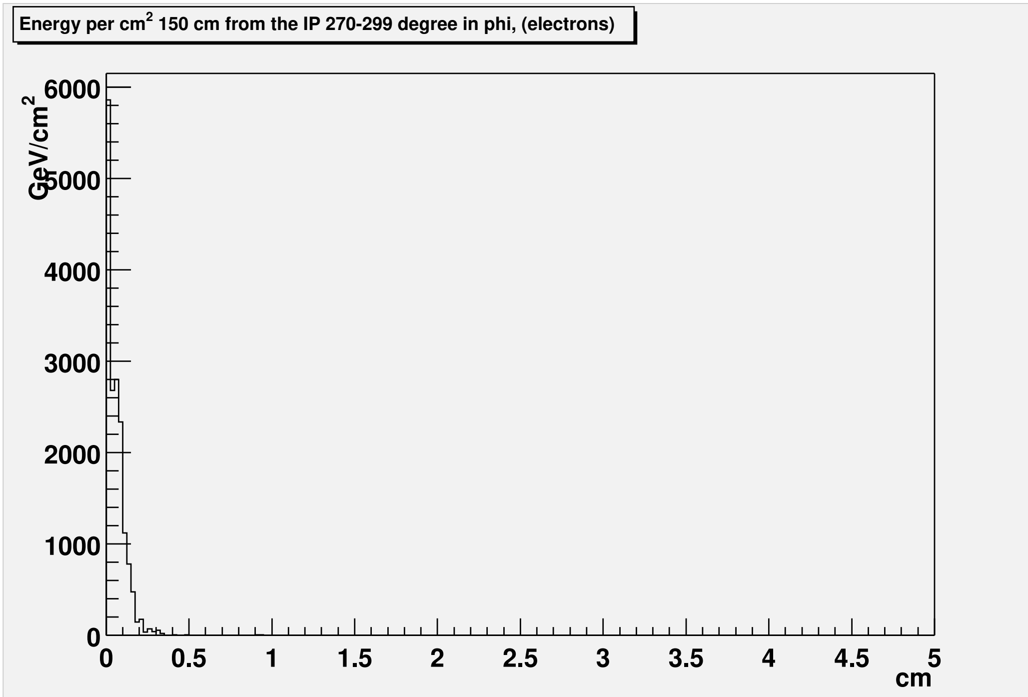

Figure 18: The energy per cm^2 deposited by electrons on a plane 150 cm in the positive direction between 270 and 300 degrees azimuthally.

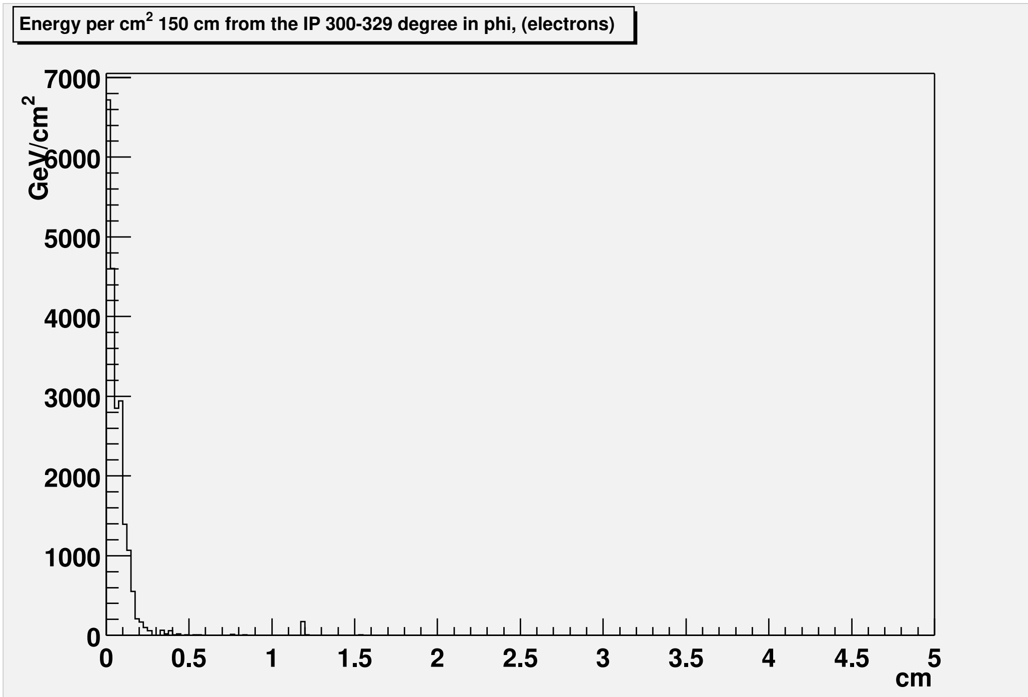

Figure 19: The energy per cm^2 deposited by electrons on a plane 150 cm in the positive direction between 300 and 330 degrees azimuthally.

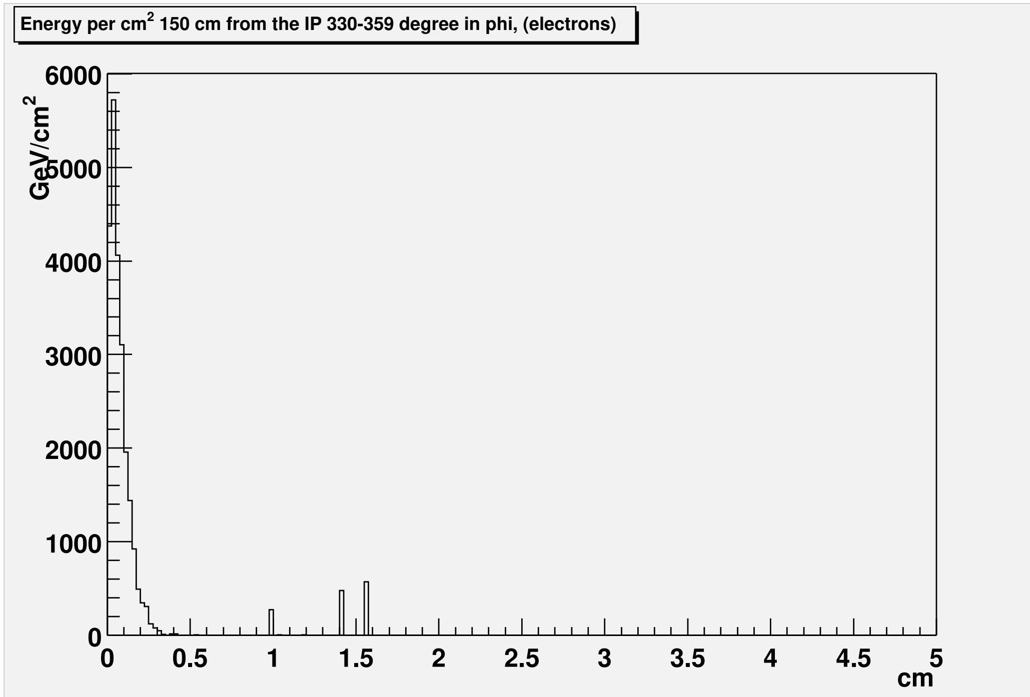

Figure 20: The energy per cm^2 deposited by electrons on a plane 150 cm in the positive direction between 330 and 360 degrees azimuthally.

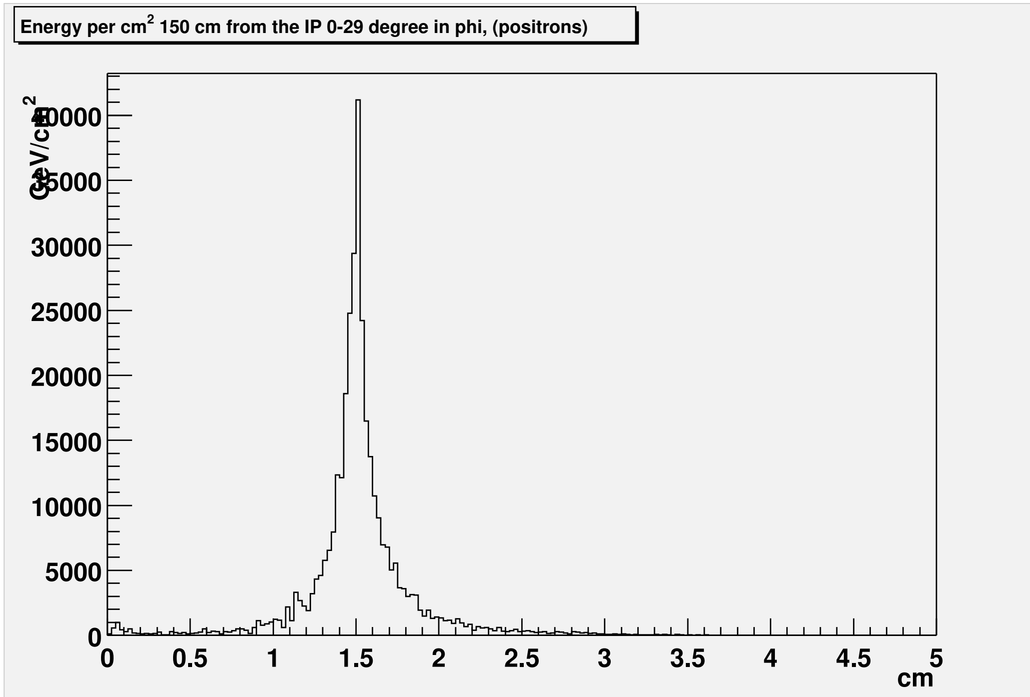

Figure 21: The energy per cm^2 deposited by positrons on a plane 150 cm in the positive direction between 0 and 30 degrees azimuthally.

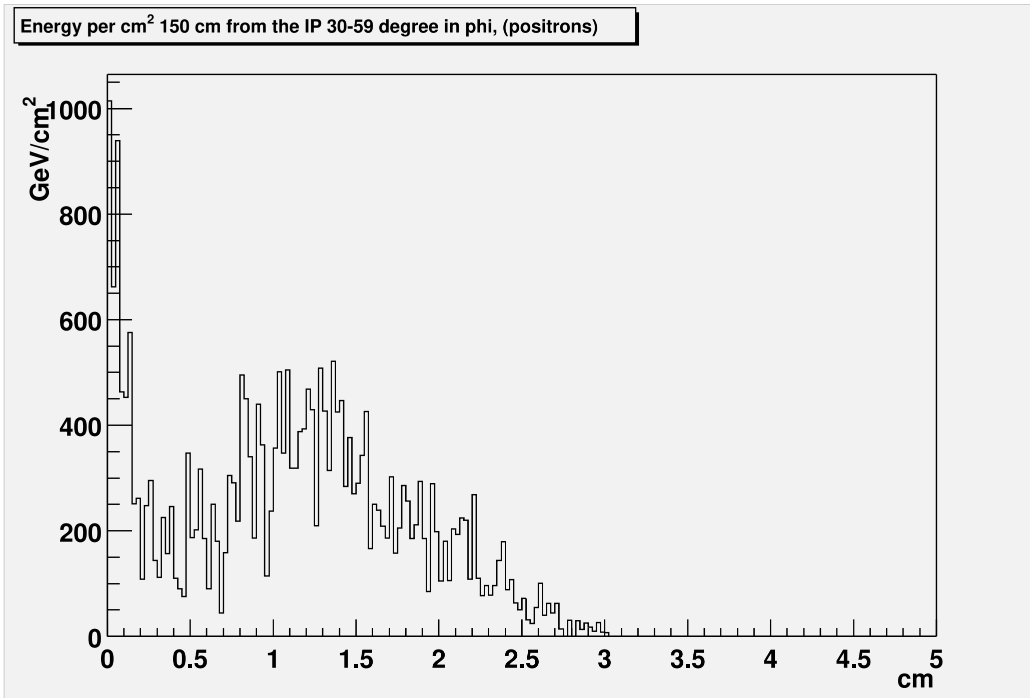

Figure 22: The energy per cm^2 deposited by positrons on a plane 150 cm in the positive direction between 30 and 60 degrees azimuthally.

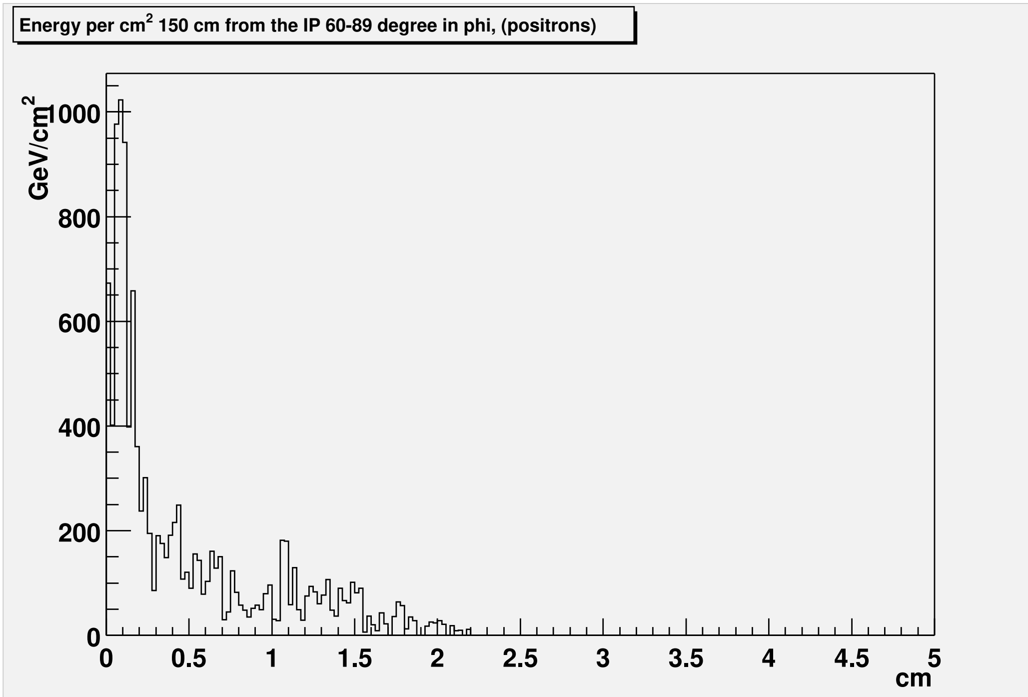

Figure 23: The energy per cm^2 deposited by positrons on a plane 150 cm in the positive direction between 60 and 90 degrees azimuthally.

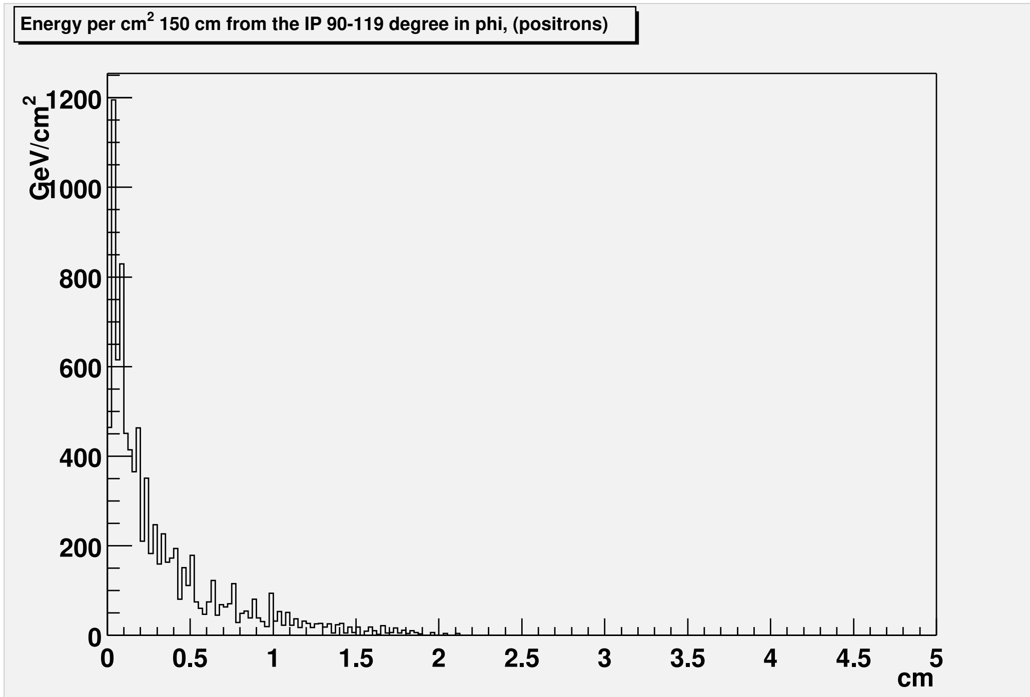

Figure 24: The energy per cm^2 deposited by positrons on a plane 150 cm in the positive direction between 90 and 120 degrees azimuthally.

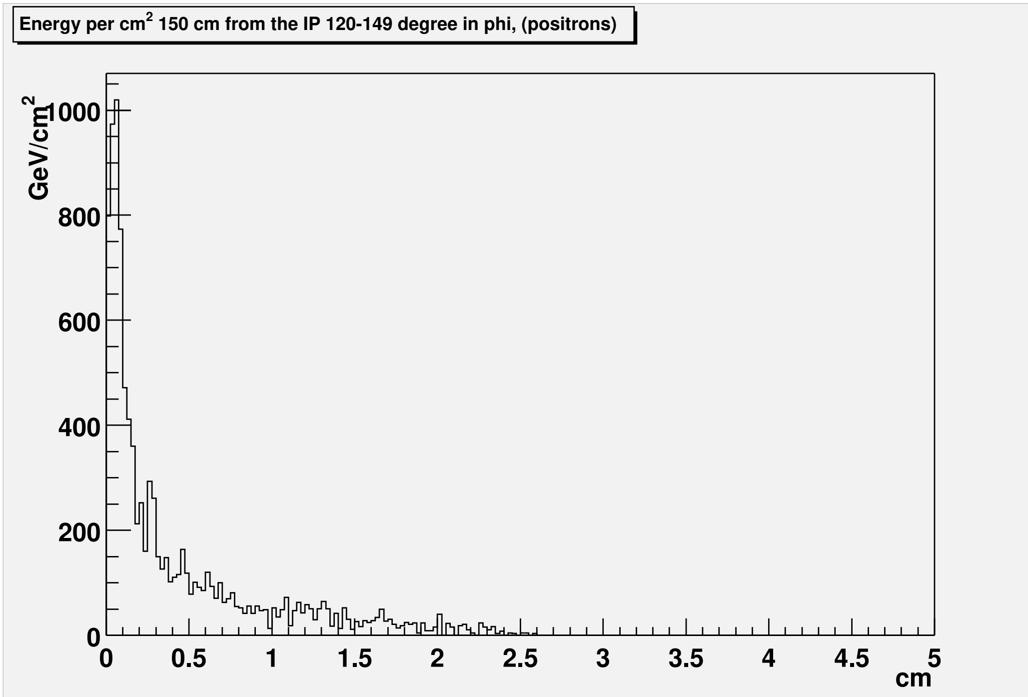

Figure 25: The energy per cm^2 deposited by positrons on a plane 150 cm in the positive direction between 120 and 150 degrees azimuthally.

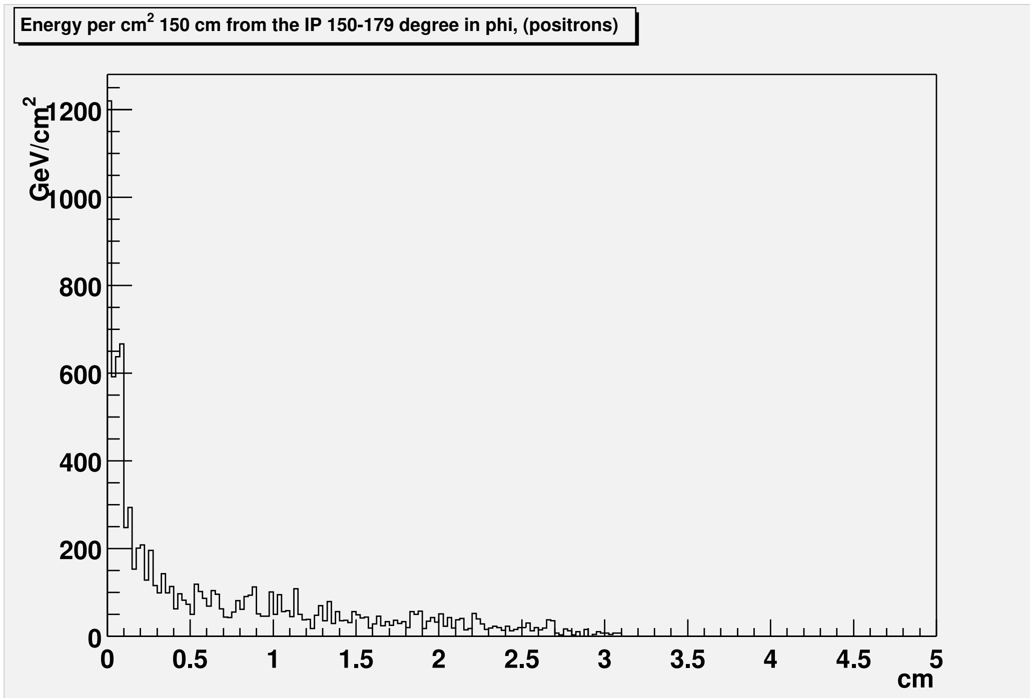

Figure 26: The energy per cm^2 deposited by positrons on a plane 150 cm in the positive direction between 150 and 180 degrees azimuthally.

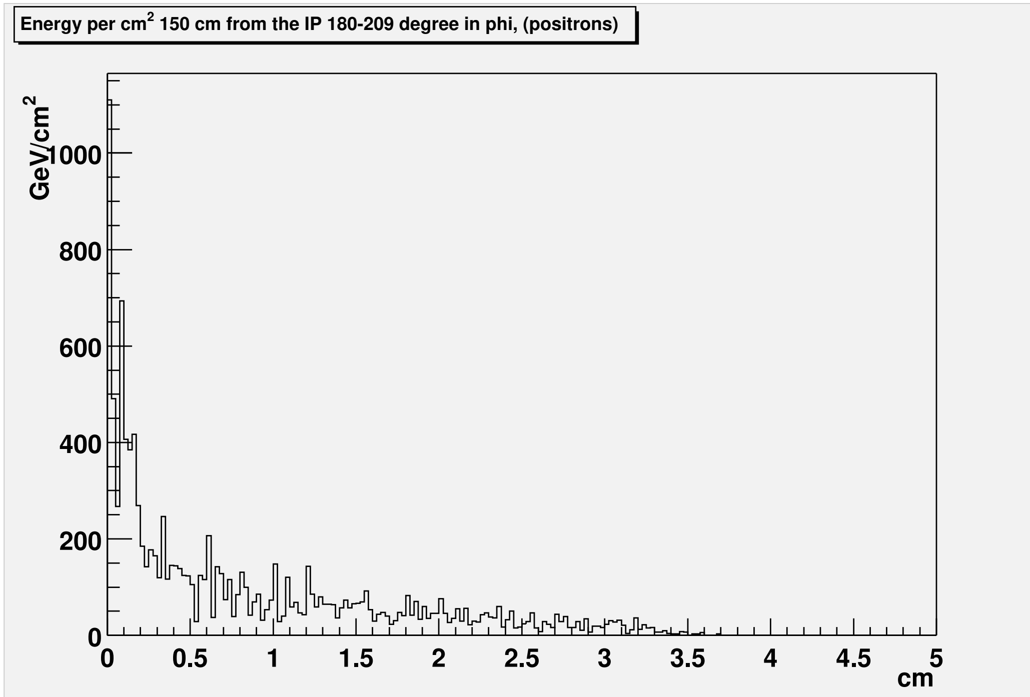

Figure 27: The energy per cm^2 deposited by positrons on a plane 150 cm in the positive direction between 180 and 210 degrees azimuthally.

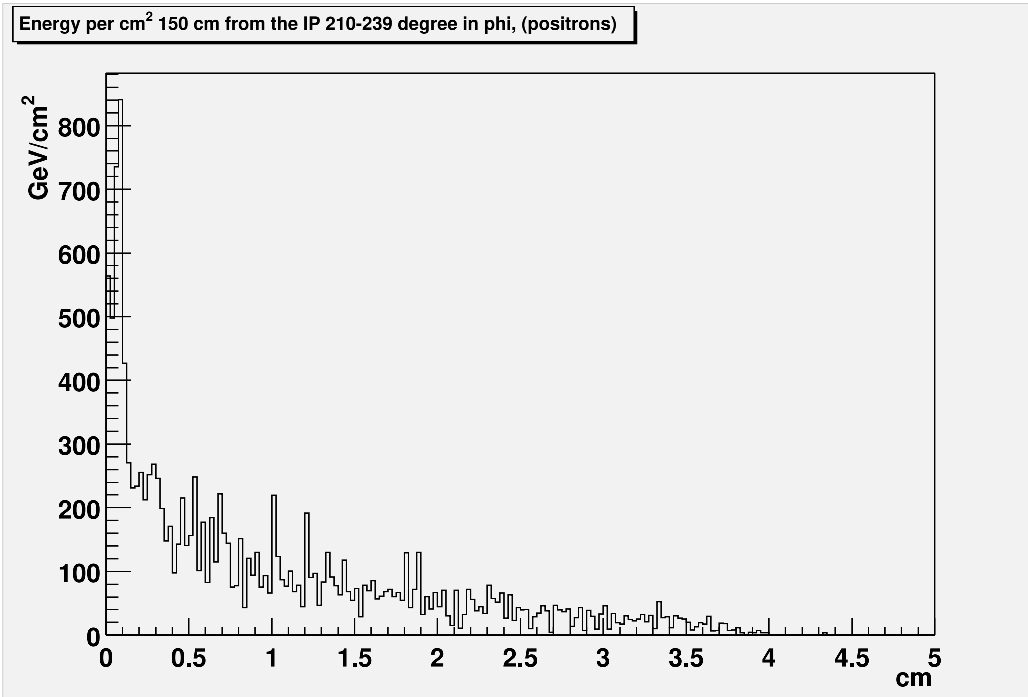

Figure 28: The energy per cm^2 deposited by positrons on a plane 150 cm in the positive direction between 210 and 240 degrees azimuthally.

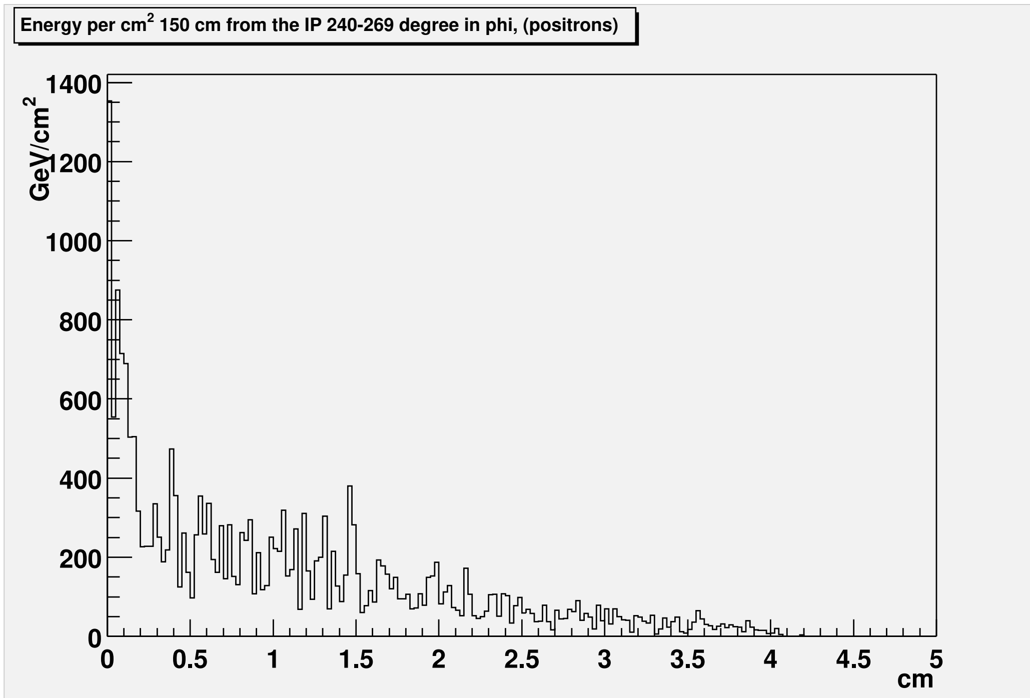

Figure 29: The energy per cm^2 deposited by positrons on a plane 150 cm in the positive direction between 240 and 270 degrees azimuthally.

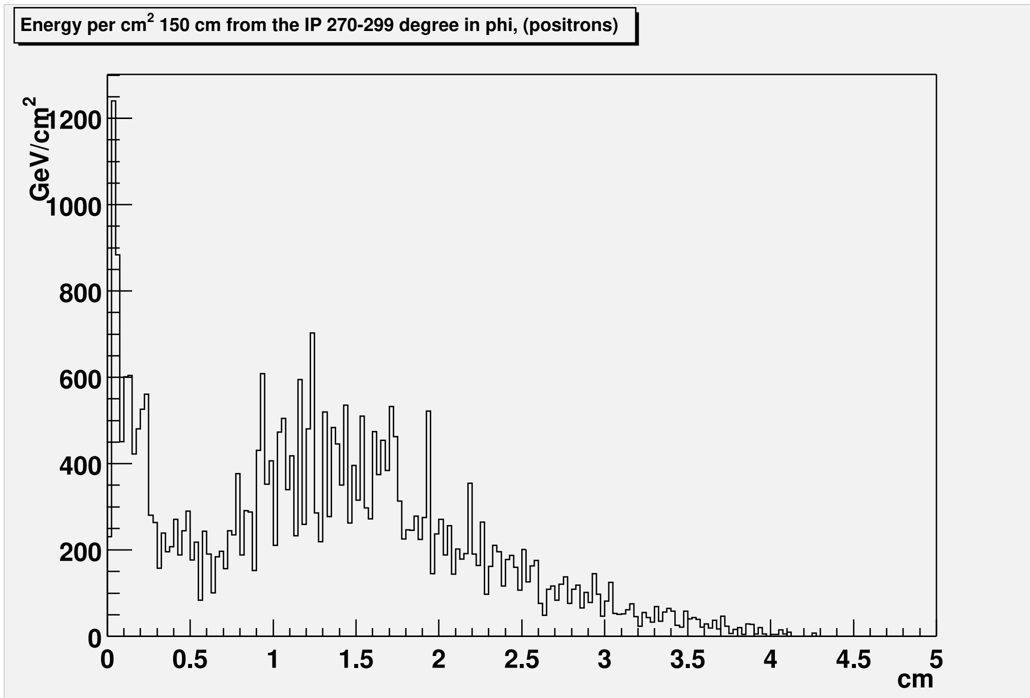

Figure 30: The energy per cm^2 deposited by positrons on a plane 150 cm in the positive direction between 270 and 300 degrees azimuthally.

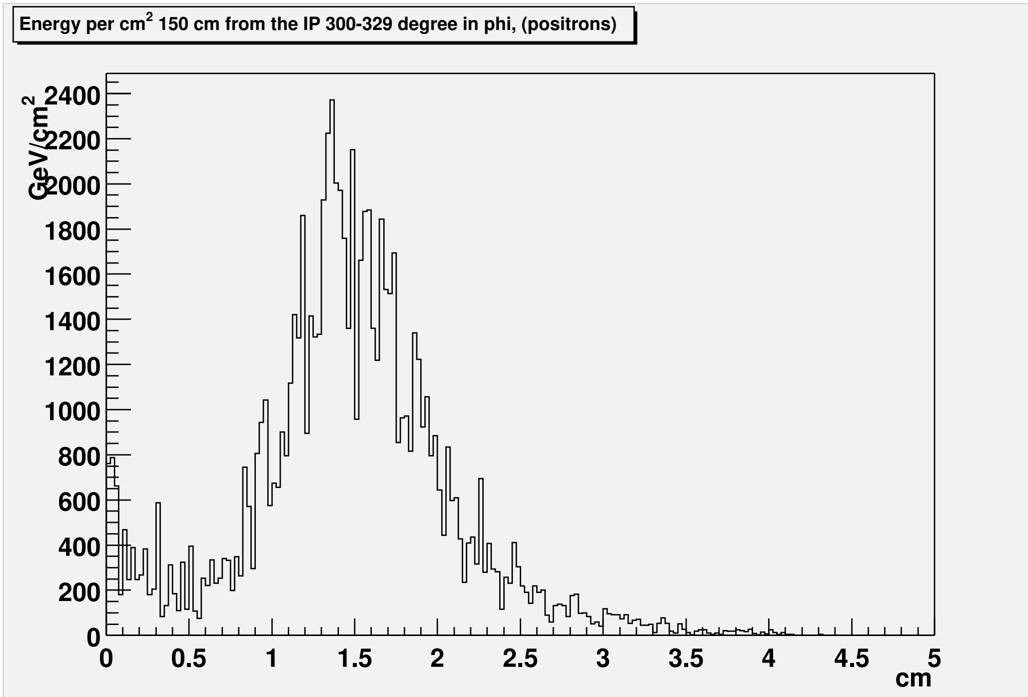

Figure 31: The energy per cm^2 deposited by positrons on a plane 150 cm in the positive direction between 300 and 330 degrees azimuthally.

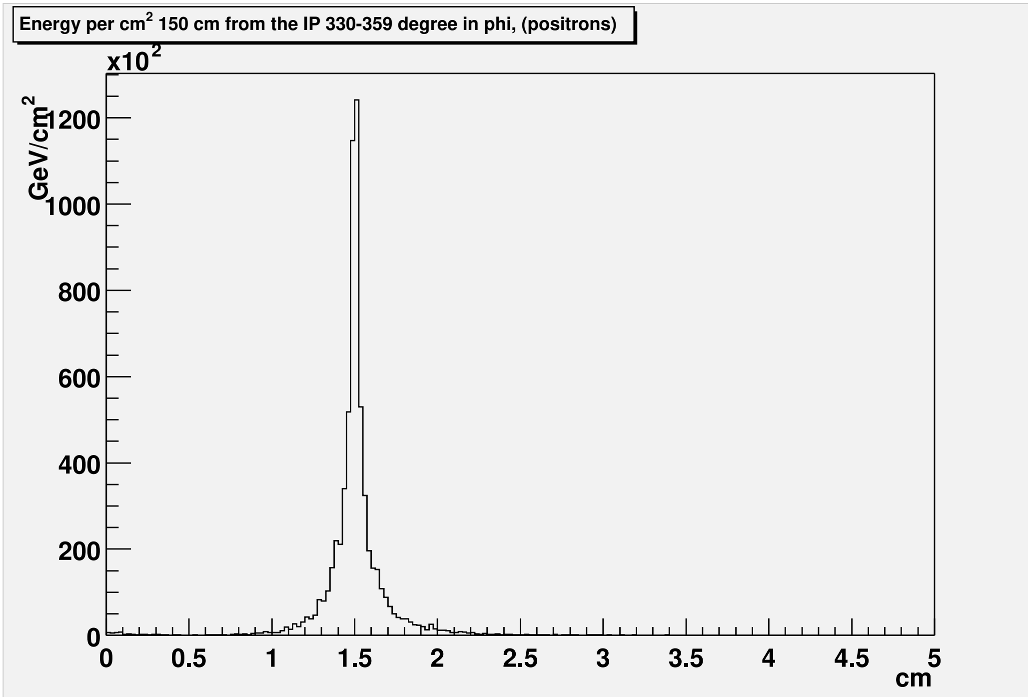

Figure 32: The energy per cm^2 deposited by positrons on a plane 150 cm in the positive direction between 330 and 360 degrees azimuthally.

7 Conclusions

A detector that can see down to the tens of mrad range may help to eliminate the two photon background that can cause problems for the study of Supersymmetry. The problem with building such a detector is the large amount of beam-produced radiation that appears at these small angles. Of the different forms of this radiation, the primary beam particles, bremsstrahlung, beamsstrahlung, and bhabha particles most likely will not hinder our search. Pair-produced electrons and positrons, however, have a large enough angular distribution that they might interfere with our search. The number of incident particles in the region of interest (greater than 30 mrad) may be large enough to obscure any signal we may be looking for, depending on the strength of the magnetic field used. With a 6 T magnetic field, virtually none of the pair-produced particles are left at greater than 30 mrad. In addition, the energies of these particles are only a few GeV at most, suggesting that it will possible to separate at angles greater than 25 mrad, these low-energy pair-produced particles from the particles generated by two-photon events, which are the particles of interest.

References

[1] Danielson, N. and Goodman, L., "Point 2 Selectrons and the Standard Model Background." University of Colorado, COLO HEP 422. 1998.

[2] Danielson, N., "Search for Supersymmetry and the Two Photon Background." University of Colorado, COLO HEP 423. 1998.

[3] Schulte, D. in Appendix A of "Study of Electromagnetic and Hadronic Background in the interaction region of the TESLA Collider." University of Hamburg, unpublished. 1996, http://www.slac.stanford.edu/~twmark/nlc/GUINEA_PIG/.

[4] S. Kuhlman *et al.*, *Physics and Technology of the Next Linear Collider*, BNL 52-502, Fermilab-PUB-96-112, LBNL-PUB-5425, SLAC Report 485, UCRL-ID-124160, submitted to the Snowmass '96 conference, p. 11. 1996.